

## 16.4 A CMOS Interface for a Gas-Sensor Array with a 0.5%-Linearity over 500k $\Omega$ -to-1G $\Omega$ Range and $\pm 2.5^\circ\text{C}$ Temperature Control Accuracy

M. Malfatti<sup>1</sup>, D. Stoppa<sup>1</sup>, A. Simoni<sup>1</sup>, L. Lorenzelli<sup>1</sup>, A. Adami<sup>1</sup>, A. Baschiroto<sup>2</sup>

<sup>1</sup>Center for Scientific and Technological Research, Trento, Italy

<sup>2</sup>University of Lecce, Lecce, Italy

Recent gas sensor applications (like wine recognition for the proposed device) require the development of efficient gas detector systems. A gas-detector system is composed of a sensor module, an electronics read-out (including the heater and the temperature control for the microsensor substrate) and a post processor. These parts work together and the gas detector performance can be improved by optimizing the system from a top-down point of view. Several techniques are now under development to improve the detector selectivity and sensitivity. A promising one, which combines an array of sensors and a temperature gradient approach [1], is applied to the sensor structure illustrated in Fig. 16.4.1. Each of the eight metal-oxide (MOX) semiconductor gas sensors in the array consists of a sensitive layer (WO<sub>3</sub>) deposited on a 1 $\mu\text{m}$ -thick SiO<sub>2</sub>-Si<sub>3</sub>N<sub>4</sub> multilayer micromachined suspended membrane. These sensors behave electrically like resistors, whose values depend on the sensitive layer, gas concentration and operating temperature. Polysilicon heaters and temperature sensors (thermometers) have been included to obtain a flexible control and setting of the operating temperature gradient. The advantages of this approach are exploitable only with a dedicated interface, featuring:

- a sensor read-out channel that is highly linear over a large resistance range (1M $\Omega$  to 1G $\Omega$ );
- and an accurate sensor substrate temperature control ( $\pm 2.5^\circ\text{C}$  in the 100 to 400 $^\circ\text{C}$  range).

A 1% sensor resistance measurement can be performed in various ways. The area occupied and realization cost increases when sophisticated calibration systems [2] or complex control circuits [3] are used. The approach based on a resistance-to-period conversion is extremely simple, but in [4] it has insufficient linearity and is too sensitive to parasitic capacitance. An improved implementation of the read-out channel is shown in Fig. 16.4.2. The sensor bias circuit is separate from the oscillator circuit to overcome the critical limitations of the circuit in [4]. A reference voltage  $V_{IN}$  is applied to the sensor, generating a current ( $V_{IN}/R_{SENS}$ ), which is mirrored to alternately charge and discharge the capacitor  $C$ . The resulting oscillation is regulated by the switches  $SW_{UP}$  and  $SW_{DW}$ , which are driven by the Schmitt trigger. If  $R_{SENS}$  maintains a constant value during the whole integration time interval, the output signal frequency is  $f_o = V_{IN}/(2 \cdot C \cdot \Delta V \cdot R_{SENS})$ , where  $\Delta V$  is the hysteresis of the Schmitt trigger. For given values of  $V_{IN}$ ,  $C$  and  $\Delta V$ , the oscillator frequency is inversely proportional to the sensor resistance. The commutation path switches are optimized since they are the main sources of additional delay that degrades the frequency measurement accuracy. The read-out channel is calibrated, in terms of the baseline sensor value, by controlling the voltages  $V_{IN}$  and  $\Delta V$ , and the integration capacitor  $C$  (a digitally-controlled capacitor array from 0.5 to 62.5pF with 2pF steps). The digital output oscillation frequency (representing the gas sensor's resistance value) is counted with a 20MHz reference clock. Thus a 0.5% measurement accuracy requires an oscillation frequency around 5kHz for any  $R_{SENS}$  value, which is obtained by the calibration.

The heaters and the thermometers behave like resistors whose values depend on the temperature as  $R = R_{amb} \cdot (1 + TCR \cdot (T - T_{amb}))$ , where  $R_{amb}$  is the resistance value at ambient temperature  $T_{amb}$  and  $TCR$  is the thermal coefficient of resistance. The tem-

perature control circuit of Fig. 16.4.3 is based on a relaxation oscillator and takes advantage of the thermal constant of the heater-thermometer system to implement an ON/OFF control that reduces the power consumption of the circuits. The thermometer  $R_t$  and a reference resistance  $R_{REF}$  are connected as the upper-half of a Wheatstone bridge, biased with a 100 $\mu\text{A}$  maximum current flowing through  $R_t$  to avoid sensor self-heating. The unbalanced bridge current (due to  $R_t$  variations) is integrated by the feedback capacitor and generates a rectangular waveform at the comparator output. This signal drives the power MOSFET connected to the heater. The system temperature oscillates around the desired value with a correspondent  $R_t$  resistance variation around the fixed value  $R_{REF}$ . The bounding values of the oscillation depend on the loop bandwidth, which is fixed by the thermal time constant of the heater-thermometer system. External resistors in the Wheatstone bridge are used to guarantee a higher precision and  $R_{REF}$  sets the desired operating temperature of the system. The external power MOSFET is used to supply the 100mW necessary to obtain the required maximum temperature of 400 $^\circ\text{C}$ . This sensor and the electronic interface configuration have the ability to set both the temperature gradient and the temperature range, which makes the gas sensor system suitable for future applications such as detectors in chromatographic systems.

The gas sensor front-end is realized in standard 0.35 $\mu\text{m}$  CMOS 2P4M technology. The die area of the chip (shown in Fig. 16.4.7) is about 1.8mm<sup>2</sup>. The full system includes 8 read-out channels and 2 temperature control systems, as required by the target sensor system. A single read-out channel consumes 3.1mW and the temperature control circuit uses 0.65mW, both from a single 3.3V supply.

Figure 16.4.4 shows the linearity error versus the sensor resistance value; note that the linearity is achieved by fully exploiting the calibration capability. A 0.5% measurement accuracy is obtained for sensor resistance in the 500k $\Omega$  to 1G $\Omega$  range. The SNR is higher than 48dB in the entire resistance range (Fig. 16.4.5), giving a 114dB DR.

The temperature control circuit is validated using a single heater-thermometer device developed with the same material and technology process as will be used for the array. Fig. 16.4.6 shows the waveform, acquired with the oscilloscope, of the comparator's output signal and the voltage at node A (see Fig. 16.4.3). The  $\pm 5\text{mV}$  voltage oscillation  $\Delta V_A$  corresponds to a  $\pm 10^\circ\text{C}$  temperature oscillation around the target value of 250 $^\circ\text{C}$ . The sensor used for the test, however, presents a time-constant (6ms) 4 times shorter than the time constant predicted for the final sensor. This time constant produces a temperature oscillation larger than the final one will be. Thus, with the final sensor, the expected oscillation is about  $\pm 2.5^\circ\text{C}$ , which is competitive with the control precision achieved with a much more complex solution [3].

### References:

- [1] A. Adami et al., "Microhotplate-Based Silicon Gas Sensor Arrays with Linear Temperature Gradient for Wine Quality Monitoring," *Proc. SPIE*, Vol. 5836, pp. 686-695, 2005.
- [2] M. Grassi et al., "A 0.1% Accuracy 100 $\Omega$ -20M $\Omega$  Dynamic Range Integrated Gas Sensor Interface Circuit with 13+4 Bit Digital Output," *Proc. ESSCC*, pp. 351-354, 2005.
- [3] D. Barretino et al., "A Single-Chip CMOS Micro-Hotplate Array for Hazardous-Gas Detection and Material Characterization," *IEEE ISSCC Dig. Tech. Papers*, pp. 312-313, Feb., 2004.
- [4] A. Flammini et al., "A Low-Cost Interface to High-Value Resistive Sensor Varying Over a Wide Range," *IEEE T. Instrum. and Meas.*, Vol. 53, no. 4, pp. 1052-1056, 2004.

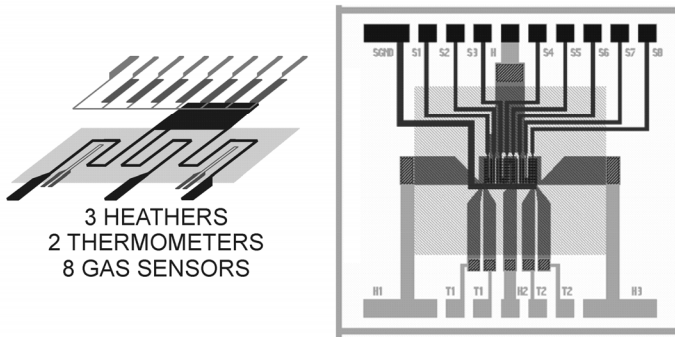


Figure 16.4.1: Gas sensor architecture and layout.

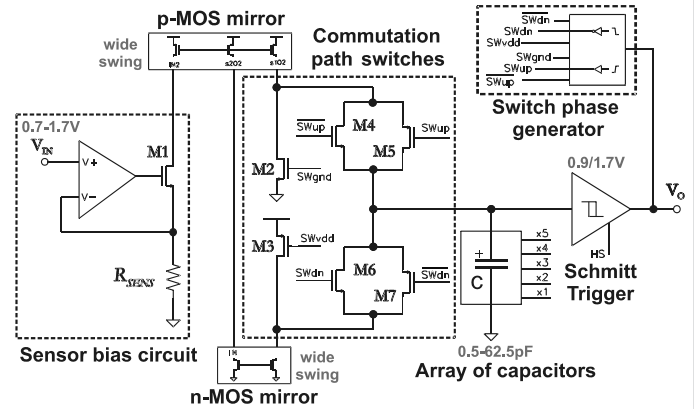


Figure 16.4.2: Principle of the gas sensor read-out circuit.

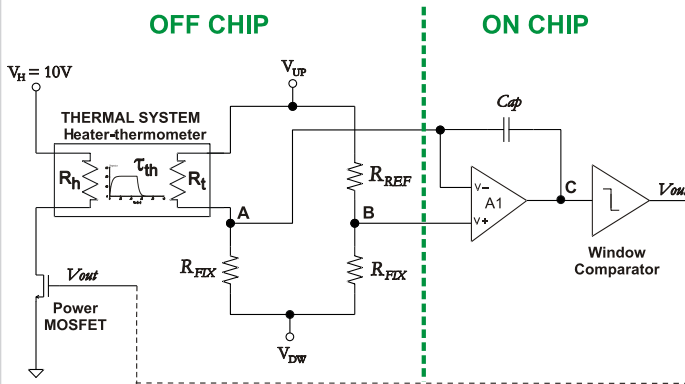


Figure 16.4.3: Temperature control circuit.

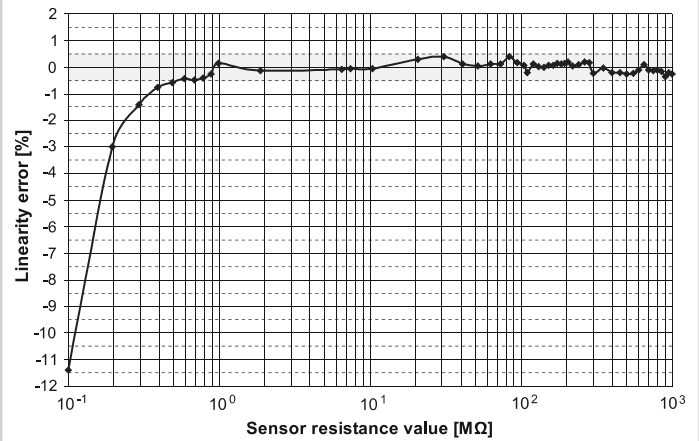


Figure 16.4.4: Measurement accuracy versus sensor resistance value.

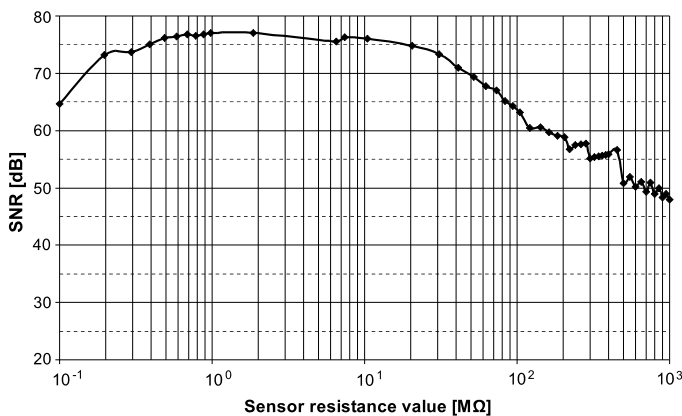


Figure 16.4.5: SNR versus sensor resistance value.

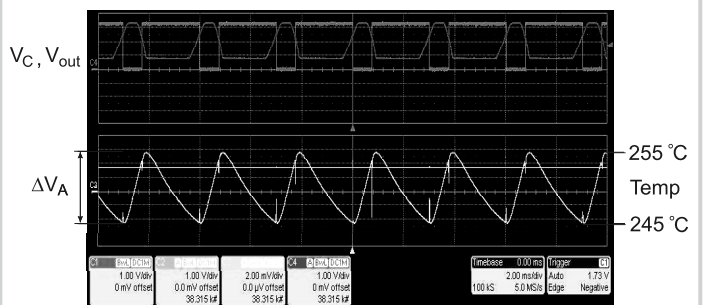


Figure 16.4.6: Thermal system temperature control.

Continued on Page 654

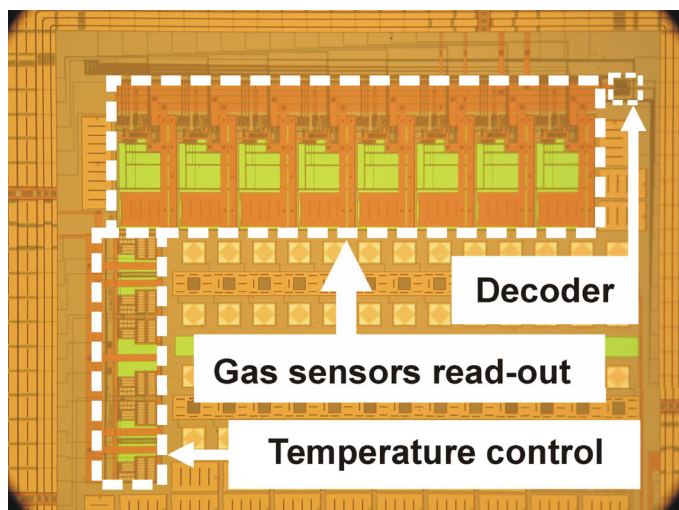


Figure 16.4.7: Chip micrograph.